Measurement of Strands Location and Inter-Strand Contact Resistance in a CIC Conductor*)

Takanori MATSUDA, Tsuyoshi YAGAI, Hidetoshi KUDO, Kazuki YOSHIDA, Tetsuhiro OBANA[1)] and Hironori MURAKAMI[2)]

Sophia University, Tokyo 102-8554, Japan
[1)]*National Institute for Fusion Science, Toki, Gifu 509-5292, Japan*
[2)]*Japan Atomic Energy Agency, Ibaraki 319-1184, Japan*

(Received 10 December 2014 / Accepted 9 April 2015)

The cable-in-conduit (CIC) conductor is the most popular one for high-field magnets installed in fusion devices. The conductor is made of hundreds of superconducting thin strands in multi stage twisted sub-cables. In spite of the current imbalance among strands resulting in degradation of conductor Ic, precise analysis of current distribution of each strand has not been done yet. In this study, we measured the strand locations and inter-strand resistance distributions which affect the current imbalance for the full-size conductor. We have investigated the resistances theoretically by using tribological analysis. It indicated that the resistance did not depend upon nominal length of distributed contact and showed the values varied by two orders of magnitude.

Keywords: super conductor, strand location, contact resistance, cable-in-conduit conductor, JT-60SA

DOI: 10.1585/pfr.10.3405067

1. Introduction

The magnets in JT-60SA are composed of cable-in-conduit conductors (CICCs) using NbTi for 18 toroidal field (TF) coils, 6 equilibrium field (EF) coils and Nb3Sn for 4 stacked central solenoid (CS) coils [1,2]. The conductors have been developed and tested to confirm the capabilities for practical use through the measurement of current sharing temperature (Tcs) and quench test [3, 4]. Because the field changing rate is faster than that of ITER, the measured AC loss was large while the temperature margin was satisfied the operating condition [2].

In the recent trend, the CICCs are designed toward the low void fraction to increase the conductor current density and to prevent the wire movement which causes Tcs degradation. Regarding the AC loss, the dominant one is coupling loss which would be enhanced in the low void fraction conductors. To decrease the loss, Although the strands have been coated with the relatively high resistance metal such as Cr or Ni, the increment of the loss was unavoidable [5]. In terms of the quantitative analysis of the loss, many groups have investigated theoretically and experimentally by using rough modelling or simplified experimental conditions. For the further quantitative investigation of the loss and the current imbalance, it is definitely needed to obtain the entire strand traces and inter-strand contact resistance distributions of full-size conductor.

We have been developed the strand traces and local inter-strand resistance measurement device in cryogenic temperature for the detail investigation of coupling loss. In this paper, we report the theoretical analysis of inter-strand resistance by using tribological study and measured inter-strand resistance in EF-L conductor by under progressing device cooled by liquid nitrogen.

2. Theoretical Background

2.1 Surface roughness and real contact area

According to the report provided by J. A. Greenwood, there is no completely flat surface of any material. Therefore, now two bodies face each other, real area of contact should be determined by the elastic and plastic deformation of their highest asperities [6,7]. Although not a few researchers tried to calculate the area of contact by applying the well-known Hertzian theory in which two spheres were coming in contact, the calculation was extremely difficult in term of two facts: one was the area of the spot of contacting two spheres depended on the radius of the asperity which was not usually known, the other was the predicted variation of area with load was proved to be incorrect. Holm tried to remove those obstacles but he did not considered the important fact of which the contact would yielded plastically far beyond elastic limit. In this paper, The load applied to the contact spot is not considered.The theory for calculating the real area of contact has already proposed by R. Buczkowski, in which the surface roughness was defined by using a stochastic model (see Fig. 1) [8]. The method is based on forming simple models describing selected specific shapes of asperities using many parameters defining micro-geometry and mechanical properties of the

author's e-mail: t.matsuda16@gmail.com
*) This article is based on the presentation at the 24th International Toki Conference (ITC24).

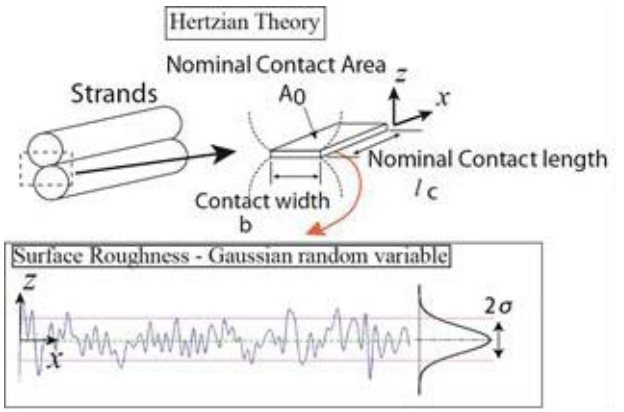

Fig. 1 Conceptual diagram of contact theories. One is Hertzian model based on the elastic theory and developed model based on microscopic random peaks with the Gaussian profile.

contacting surface. A profile of surface roughness is mathematically modeled by the random process theory. The distribution of the peaks of the surface should be typically Gaussian in which a peak is defined as a point having a greater height than the two data points on both its sides. We produce peak profiles satisfying Gaussian distribution repeatedly by using MATLAB function and make sure that the curvature which plays an important rule for calculating real area of contact has nothing to do with the horizontal resolution.

2.2 Governing equations for the estimation of real area

Now we define the discrete array of the heights of asperity as z_i (ith component) at the horizontal position of ih, where h indicates the sampling interval. First of all, we introduce the slope m and curvature as follows,

$$m = \frac{z_{i+1} - z_i}{h}, \quad \kappa = \frac{z_{i+1} - 2z_i + z_{i-1}}{h^2}. \tag{1}$$

The standard deviations of the height z, slope m and curvature κ are expressed as σ, σ_m and σ_κ, respectively. We also introduce normalized height and curvature, such as,

$$\zeta = \frac{z}{\sigma}, \quad t = -\frac{\kappa}{\sigma_\kappa}. \tag{2}$$

The minus sign of the parameter t is necessary because we are interested only in the negative values of curvature, in other words, the summits of rough surface. If the surfaces come together until their reference planes are separated by the distance d, then all asperities are in contact if height z exceeds the separation d. For preparing the contact probability evaluation, we introduce the normalized separation $\eta = d/\sigma$, then the contact probability should be described as,

$$P(\eta) \equiv \mathrm{Prob}(\zeta > \eta) = \int_\eta^\infty \int_0^\infty P_{\mathrm{peak}}(\zeta, t)\mathrm{d}\zeta\,\mathrm{d}t, \tag{3}$$

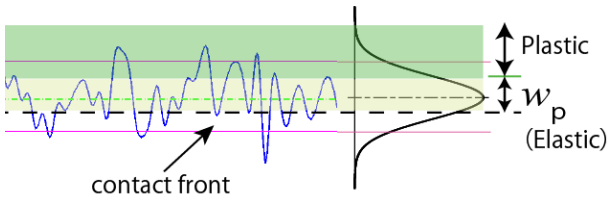

Fig. 2 Concept of contact on a rough surface. Both elastic and plastic deformations are considered based on the model provided by Buczkowski.

where,

$$P_{\mathrm{peak}}(\zeta, t) = \begin{bmatrix} P(\zeta_1, t_1) & P(\zeta_2, t_1) & \cdots & P(\zeta_n, t_1) \\ P(\zeta_1, t_2) & \ddots & & \\ \vdots & & \ddots & \\ P(\zeta_1, t_m) & \cdots & \cdots & P(\zeta_n, t_m) \end{bmatrix}. \tag{4}$$

P_{peak} is a joint probability density which satisfies following condition.

$$\sum_n \sum_m P_{\mathrm{peak}}(\zeta_n, t_m) = 1. \tag{5}$$

As Buczkowski pointed out, a normalized critical separation for the inception of plastic deformation is also needed.

$$w_p^* = \frac{E\sigma_m}{H\sigma}. \tag{6}$$

Where E is Young's modulus and H is hardness of material.

The conceptual diagram of making contact of rough surface is shown in Fig. 2.

As a brief conclusion of this section, we finally obtain the equation for calculation of the real area of contact as follows,

$$A(\eta) = \pi N\sigma \int_\eta^{\eta+w_P^*} \int_0^\infty \frac{1}{\sigma_\kappa t}(\zeta - \eta)P_{\mathrm{peak}}(\zeta, t)\mathrm{d}\zeta\,\mathrm{d}t \tag{7}$$

$$+\pi 2N\sigma \int_{\eta+w_P^*}^\infty \int_0^\infty \frac{1}{\sigma_\kappa t}\left[\zeta - \left(\eta + \frac{1}{2}w_P^*\right)\right] P_{\mathrm{peak}}(\zeta, t)\mathrm{d}\zeta\,\mathrm{d}t,$$

$$\text{where, } N = A_0 \frac{1}{2\pi}\left(\frac{\sigma_\kappa}{\sigma_m}\right)^2, \; A_0 : \text{nominal contact area.}$$

The detail discussion of these equations is not the purpose of this paper, if needed, see [8].

3. Experimental Setup

3.1 New device to measure the inter-strand resistance

Our group has been developed the measurement system of strand traces for full size CICCs. The schematic of the system is shown in Fig. 3.

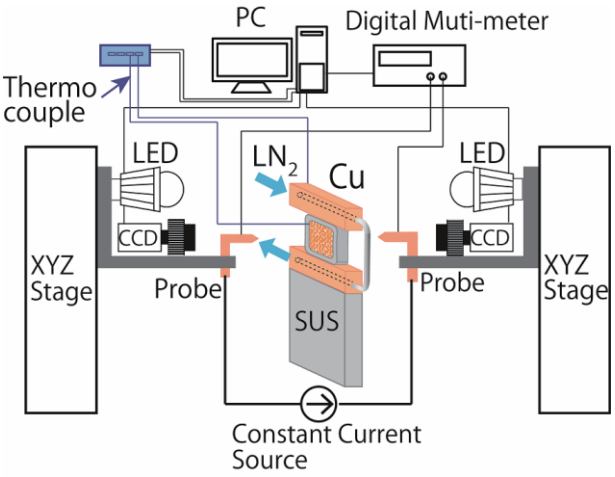

Fig. 3 Schematic of strand trace measurement system for full-size CICCs. To measure Cu strand locations, we refined the machine to lower the sample temperature by using LN_2 force-cool.

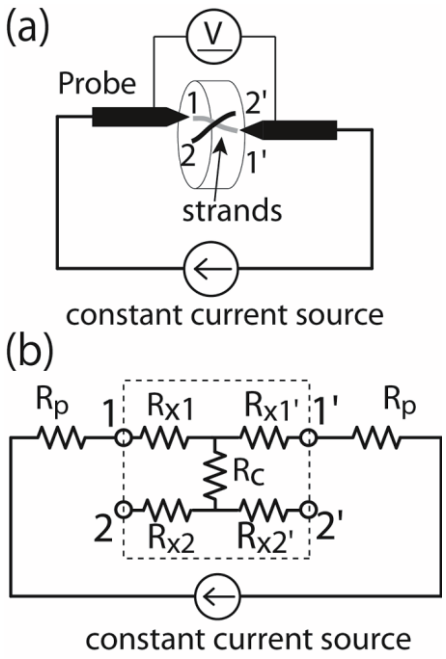

Fig. 4 Schematics of measuring strand resistance (a) and equivalent circuit model of the measurement.

Except for PC and measurement instruments, the whole system is inserted into large vacuum vessel 800 mm in diameter. The sample which is sliced off from CICC after being hardened by epoxy is put between Cu brocks force-cooled by liquid N_2. To prevent subjecting the frost on the sample surface, the moisture around sample is perfectly controlled less than 0.3% by filling N_2 gas inside the vessel. The background pressure is also controlled from −0.08 MPa to +0.01 MPa. Typical temperature of the sample is −120 degrees in Celsius.

The principal of strand trace measurement is shown in Fig. 4. In Fig. 4 (a), the resistance between two cross sections of one or two strands is measured by using four-terminal method. Figure 4 (b) describes the equivalent circuit of the resistance measurement. The resistance between cross section 1 and 1' might be less than that between 1 and 2'. In this case, the resistance is just the strand resistance which is corresponds to the resistance of a cylinder. Then, the strand location on both left and right side of the sample is identified.

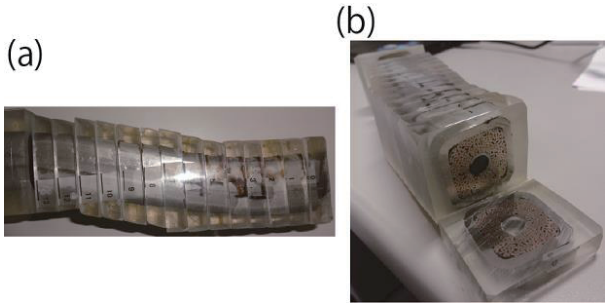

Fig. 5 Pictures of slice EF-L conductor. The top view is (a) and enlargement of a cross section is (b). The hardening by epoxy is needed for preventing the strand movement during cutting the conductor.

Table 1 Specifications of EF-L Conductor.

	EF-L
Strand Material (Number of Strands)	NbTi (216) and Cu (108)
Surface Coating (thickness)	Ni (2 μm)
Strand diameter	0.823 mm
Jacket outer size	25 mm × 25 mm
Void fraction	34 %

More important information in this paper is resistance between 1 and 2' or 2 and 1'. This means that we measure the inter-strand resistance per sample thickness 10 mm. To the best of my knowledge, local inter-strand resistance measurement has never been carried out. The results obtained in this measurement enable us to evaluate the current re-distribution conductance across the conductor axis.

3.2 Sample preparation

As mentioned in previous section, we need the sample CICC slices with 10 mm in thickness. We recycled CICCs for EF coils in JT-60SA having used in experiments for assessment of Tcs and AC loss. The pictures of the slice samples impregnated by epoxy are shown in Fig. 5.

Specifications of EF-L conductor are listed in Table 1.

4. Result and Discussion

4.1 Calculation results of real area of contact

Figure 6 shows the calculation results of real areas of contact as a function of the normalized separation be-

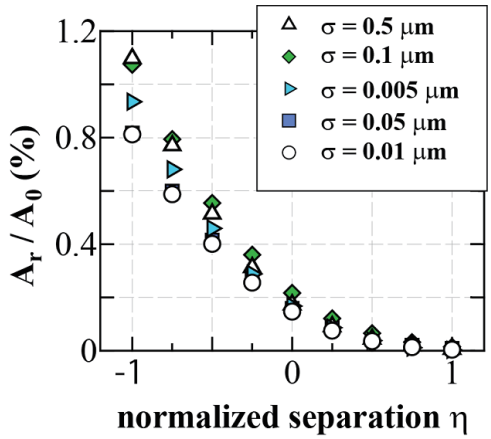

Fig. 6 Calculation results of the real contact area as a function of normalized separation η. Where Ar is real contact area.

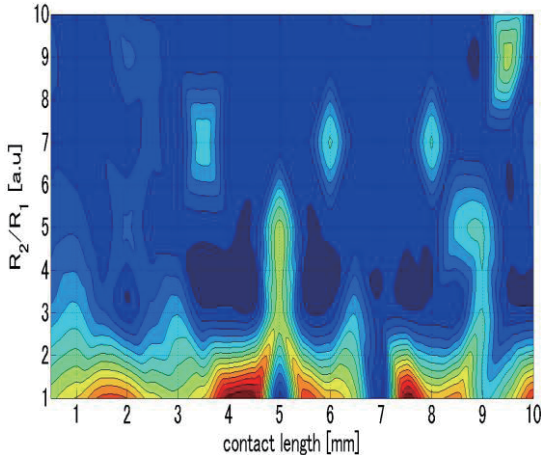

Fig. 7 Experimental results of contact resistance between strands normalized by the strand resistance as a function of nominal contact length. Only we selected the data for combinations of which strands get closed each other. Contact resistance shows many points with red and shows it with blue as there becomes few it. Where R1 is the resistance of the strand and R2 is the contact resistance.

tween surfaces of two contacting bodies. The areas shown in Fig. 6 are translated into the ratio to the nominal areas involved in (7). According to the theory provided by Buczkowski, the contact situation occurs at the normalized separation 1 and finishes at minus 1. The standard deviations of the height are selected from 0.005 μm to 0.5 μm which seem to be reasonable for the Ni coating with 2 μm in thickness.

It is a little of surprise that the maximum ratio of the real contact area is no more than 1.2% of nominal area. Besides, it was revealed that there was difference more than one order to the real contact area like that the ratio would vary from 0.1% to 1.2%, which is the range of an order of magnitude.

4.2 Measured inter-strand resistance

We measured the inter-strand contact resistance in EF-L conductor as a first step of testing our new device. Figure 7 shows the results of contact resistance normalized by the strand resistance which is also obtained in the same measurement sequence as a function of nominal contact length. The nominal contact length is determined by the locations of two strands, so the 10 mm nominal contact indicates that two strands are contacting each other throughout their length. It is clear that the range of the contact resistance is surprisingly wide for long contact length case. Though the contact head is equal, there are uneven data in measured contact resistance. Although there is not so much data so far, the several results show the big difference of an order of magnitude even the nominal contact lengths are almost the same value.

4.3 Discussion

The calculation and measured results designate that the contact resistance between strands will not be determined by their geometrical relation. Not only for the conductors used in JT-60SA but also other ones in ITER, coupling current which causes major loss in CICCs would flow through the mechanical contact surface between strands. When the normalized separation of two metal surfaces is minus one, which seems to have large deformation all over the surface, the real area of contact is only 1% of nominal area. In that case, the Cr or Ni plate for preventing higher coupling current seems to work well as reported by Ando [5].

On the other hand, the void fraction of CICCs tends to be lower than 30% for removing the anxiety of Tcs degradation during charge and discharge cycles by shorten the first twist pitch to minimize the deformation of fragile strand. The analysis of mechanism of the strand buckling has reported by our group and the other one [9]. The strands would be flattened by one fourth of diameter in low void fraction conductor. In this case, the normalized separation must be much smaller than minus one, which leads to much lower contact resistance between strands and larger loss.

5. Summary

We developed the device which was able to measure the local inter-strand resistance and investigated quantitatively the real area of contact by using tribological knowledge. The calculation of the real area of contact by assuming the surface asperities satisfied the Gaussian distribution showed that the values would be vary by an order of magnitude. The experimental results of local inter-strand resistance well agreed with the wide range difference even if the nominal contact length seemed to be almost equal. In the future work, we will quantitatively estimate the coupling loss by using strand traces and local inter-strand resistance distribution.

[1] K. Yoshida *et al.*, Physica C **470**, 1727 (2010).
[2] K. Kizu *et al.*, IEEE Trans. Appl. Supercond. **18**, no.2, 212 (2008).
[3] K. Nakamura *et al.*, IEEE Trans. Appl. Supercond. **21**, no.3, 2016 (2011).
[4] H. Murakami *et al.*, IEEE Trans. Appl. Supercond. **20**, no.3, 512 (2010).
[5] T. Ando *et al.*, J. Cryo. Soc. Jpn. **22**, 367 (1987).
[6] J.A. Greenwood, Proc. R. Soc. London A **393**, 133 (1984).
[7] J.A. Greenwood and J.B.P. Williamson, Proc. R. Soc. London A **295**, 300 (1966).
[8] R. Buczkowski and M. Kleiber, Comput. Methods Appl. Mech. Eng. **169**, 43 (1999).
[9] T. Yagai *et al.*, IEEE Trans. Appl. Supercond. **24,** no.3, 8800404 (2014).